Finite temperature transition for 2-flavor lattice QCD at finite isospin density

J. B. Kogut[1] and D. K. Sinclair[2]

[1]*Dept. of Physics, University of Illinois, 1110 West Green Street, Urbana, Illinois 61801-3080, USA*
[2]*HEP Division, Argonne National Laboratory, 9700 South Cass Avenue, Argonne, Illinois 60439, USA*

(Received 23 July 2004; published 4 November 2004)

We simulate 2-flavor lattice QCD at finite isospin chemical potential μ_I, for temperatures close to the finite temperature transition from hadronic matter to a quark-gluon plasma. The μ_I dependence of the transition coupling is observed and used to estimate the decrease in the transition temperature with increasing μ_I. These simulations are performed on an $8^3 \times 4$ lattice at three different quark masses. Our estimate of the magnitude of the fluctuations of the phase of the fermion determinant at small quark-number chemical potential μ, suggest that the position of the small μ and small μ_I transitions should be the same for $\mu_I = 2\mu$, and we argue that the nature of these transitions should be the same. For all $\mu_I < m_\pi$ the smoothness of these transitions and the values of the Binder cumulant B_4, indicate that these transitions are mere crossovers, and show no sign of a critical endpoint corresponding to that expected at finite μ. This suggests that this finite μ critical endpoint, if it exists, lies at $\mu > m_\pi/2$ over the considered range of quark masses. For $\mu_I > m_\pi$ and a small isospin (I_3) breaking term λ, we do find evidence of a critical endpoint which would indicate that, for $\lambda = 0$, there is a tricritical point on the phase boundary where the pion condensate evaporates, where this phase transition changes from second to first-order.

DOI: 10.1103/PhysRevD.70.094501 PACS numbers: 11.15.Ha, 11.10.Wx, 12.38.Gc, 12.38.Mh

I. INTRODUCTION

QCD at finite baryon-/quark-number density describes nuclear matter. Beyond nuclei it describes the physics of neutron stars and has the potential to predict such exotic objects as quark stars. Hot hadronic matter at low baryon-number density was present in the early universe. Relativistic heavy-ion collisions at RHIC and CERN produce hot nuclear matter.

QCD at a finite chemical potential μ for quark-number, has a complex fermion determinant, which makes the naive application of standard lattice simulation methods, which are based on importance sampling, difficult if not impossible. To circumvent these problems people have introduced various schemes which are applicable to high temperatures and small μ. These include various reweighting techniques [1–3], and methods which expand physical observables as power series in μ [4–10] or related parameters [11].

Another approach is to study theories which are expected to possess some of the properties of QCD at finite μ, but have real positive fermion determinants, making them amenable to standard simulation methods. One such theory is QCD at finite chemical potential μ_I for isospin (I_3). This theory has been studied both by effective (chiral) Lagrangian techniques [12,13], as well as by direct lattice simulations [14]. At zero temperature these studies indicate that this theory undergoes a second-order phase transition with mean-field critical exponents at $\mu_I = m_\pi$, to a state characterized by a charged pion condensate which breaks I_3 spontaneously.

We report here a study of 2-flavor lattice QCD at finite μ_I and finite temperature (T), in the neighborhood of the finite temperature transition from hadronic matter to a quark-gluon plasma. Figure 1(a) is a sketch of the phase diagram in the (μ_I, T) plane, which is based on this and previous work. Since we work at finite quark mass to make the pion massive and thus to move pion condensation to finite μ_I, the finite temperature transitions form a line of crossovers emanating from the $\mu_I = 0$ transition, for small μ_I. This is indicated by the dashed line in the figure. The solid lines show the phase boundary of the superfluid phase mentioned in the previous paragraph. We calculate the position of this crossover as a function of μ_I on an $8^3 \times 4$ lattice for three different quark masses ($m = 0.05, 0.1, 0.2$), from the peaks of the susceptibilities of the various observables, using Ferrenberg-Swendsen reweighting to interpolate between the β values used in our simulations. For $\mu_I < m_\pi$, we set the symmetry breaking parameter $\lambda = 0$. From estimations of the fluctuations of the phase of the fermion determinant for small quark-number chemical potential μ we shall argue that there is an appreciable range of μ over which these fluctuations are small enough that the position of the crossover at finite μ will be the same as that at finite μ_I with $\mu_I = 2\mu$. We therefore show a simplified version of the corresponding phase diagram in the (μ, T) plane in Fig. 1(b). We find good agreement with the μ dependence of this transition observed by de Forcrand and Philipsen [6]. This agreement between the μ and μ_I dependence of the transition $\beta = 6/g^2$ and hence temperature was noted by the Bielefeld-Swansea group [4]. We also find that the transition for each of our three masses appears to remain a crossover with no sign of a critical endpoint corresponding to that expected at finite μ (shown as an open circle in Fig. 1(b), where the line of crossovers changes to a line of first-order transitions) for all $\mu_I < m_\pi$. Preliminary re-

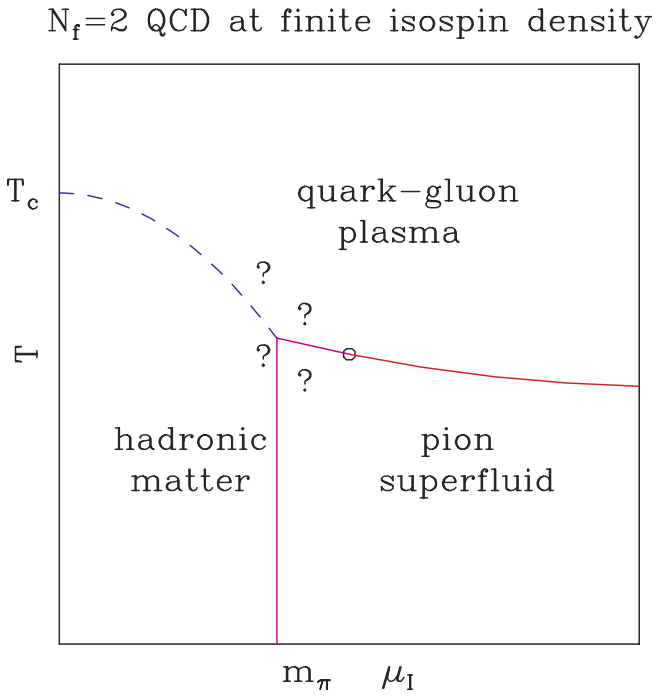

FIG. 1 (color online). (a) The proposed phase diagram for 2-flavor QCD in (μ_I, T) plane. (b) The proposed phase diagram for 2-flavor QCD in (μ, T) plane. In both cases dashed lines are crossovers, solid lines are phase transitions

sults from these simulations have been presented at conferences [15–17].

We have also studied the finite temperature transition for $\mu_I > m_\pi$. Here, for symmetry breaking parameter $\lambda = 0$, the pion condensate evaporates at the finite temperature transition, which is thus a true phase transition. However, since here the fermion propagator becomes singular (at least in the infinite volume limit) for temperatures below this transition, because of the Goldstone boson associated with the spontaneous breaking of I_3, we are forced to work at finite (small) λ, where the transition again becomes a crossover. Here we shall present evidence for a critical endpoint beyond which the transition becomes first-order. Because λ is small, we shall argue that this first-order behavior persists to $\lambda = 0$. At $\lambda = 0$, the finite temperature crossover is replaced by a second-order transition, the first-order transition remains first-order and the critical endpoint becomes a tricritical point. Although most of our simulations were performed on $8^3 \times 4$ lattices, we performed some simulations on $16^3 \times 4$ lattices close to the critical endpoint. In Fig. 1(a) the open circle on the phase boundary of the superfluid region represents this tricritical point. To the left the phase transition is second-order; to the right it is first-order.

We should contrast this high μ_I behavior, with the high μ behavior shown in Fig. 1(b). At finite μ, the first transition at $T = 0$ is expected to occur just below $m_N/3$, rather than at $m_\pi/2$. Thus the phase diagram does not collapse in the chiral limit. The line of finite temperature transitions involves chiral symmetry restoration in this limit, and should therefore cross the $T = 0$ axis beyond the domain of normal nuclear matter. Whether this line should mark the boundary of the suggested color-superconducting phase at small T is a matter for conjecture.

In Section II, we introduce lattice QCD at finite μ_I. In Section III we define the fourth-order Binder cumulants which we use to study the nature of the transitions. Section IV describes our simulations and results for small μ_I ($\mu_I < m_\pi$). The large μ_I simulations and results are presented in Section V. Section VI contains discussions and conclusions.

II. LATTICE QCD AT FINITE μ_I

The staggered quark action for lattice QCD at finite chemical potential μ_I for isospin (I_3) is

$$S_f = \sum_{\text{sites}} \left[\bar{\chi} \left(\not{\partial} \left(\frac{1}{2} \tau_3 \mu_I \right) + m \right) \chi + i \lambda \epsilon \bar{\chi} \tau_2 \chi \right], \quad (1)$$

where $\not{\partial}(\frac{1}{2}\tau_3\mu_I)$ is the standard staggered quark transcription of $\not{\partial}$ with the links in the $+t$ direction multiplied by $\exp(\frac{1}{2}\tau_3\mu_I)$ and those in the $-t$ direction multiplied by $\exp(-\frac{1}{2}\tau_3\mu_I)$. The term proportional to λ is an explicit $I_3 = \frac{1}{2}\tau_3$ symmetry breaking term. This term serves two purposes. Firstly, such a term is necessary if one is to see evidence for spontaneous I_3 breaking on a finite lattice. Secondly, it prevents the Dirac operator from becoming singular, as we see below. τ_1, τ_2 and τ_3 are the isospin matrices so that this Dirac operator is a 2×2 matrix in isospin space. The determinant

$$\det\left[\not{p}\left(\frac{1}{2}\tau_3\mu_I\right) + m + i\lambda\epsilon\tau_2\right] = \det\left[\mathcal{A}^\dagger\mathcal{A} + \lambda^2\right], \tag{2}$$

where

$$\mathcal{A} \equiv \not{p}\left(\frac{1}{2}\mu_I\right) + m, \tag{3}$$

is a 1×1 matrix in isospin space, which means that we only need use a single flavor-component fermion field in our simulations. This determinant is real and positive allowing us to use standard hybrid molecular-dynamics simulations, with noisy fermions to allow us to tune the number of flavors from eight down to 2.

We note that, for $\lambda = 0$, the determinant of Eq. (2) is just the magnitude of the determinant for 8-flavor lattice QCD with quark-number chemical potential

$$\mu = \frac{1}{2}\mu_I. \tag{4}$$

Observables for this theory include the chiral condensate,

$$\langle\bar{\psi}\psi\rangle \Leftrightarrow \langle\bar{\chi}\chi\rangle, \tag{5}$$

the charged pion condensate

$$i\langle\bar{\psi}\gamma_5\tau_2\psi\rangle \Leftrightarrow i\langle\bar{\chi}\epsilon\tau_2\chi\rangle, \tag{6}$$

and the isospin density

$$j_0^3 = \frac{1}{V}\left\langle\frac{\partial S_f}{\partial\mu_I}\right\rangle. \tag{7}$$

We will also be interested in the Wilson Line (Polyakov Loop), and the plaquette observable

$$\text{PLAQUETTE} = S_\Box = 1 - \frac{1}{3}\text{ReTr}U_\Box. \tag{8}$$

III. FOURTH-ORDER BINDER CUMULANTS

If X is an observable, its 4-th order Binder cumulant is defined by

$$B_4 = \frac{\langle(X - \langle X\rangle)^4\rangle}{\langle(X - \langle X\rangle)^2\rangle^2}, \tag{9}$$

which approaches a universal value at a critical point [18]. It has been pointed out if one chooses X to be an eigenvector of the critical scaling Hamiltonian, B_4 will be as close as is possible to its infinite volume limit on finite volumes [19]. If one plots B_4 as a function of those parameters which parametrize the departure from the critical point, the curves obtained for different lattice sizes will intersect at the critical point if X is indeed an eigenvector. For other choices of X the intersections of such curves will only tend to this unique value in the infinite volume limit. The value of the cumulant at this point of intersection will be that characteristic of the universality class of this critical point and the nature of the observable.

For transitions other than critical points, the Binder cumulant only attains its characteristic value in the infinite volume limit. For a crossover, the infinite volume value for the Binder cumulant for the order parameter is $B_4 = 3$. For a first-order transition, this Binder cumulant is $B_4 = 1$. The critical endpoint we are seeking is expected to be in the universality class of the 3-dimensional Ising model for which $B_4 = 1.604(1)$. For a mean field critical point $B_4 = \Gamma(5/4)\Gamma(1/4)/\Gamma(3/4)^2 = 2.1884\ldots$ for a 1-component order parameter [20], or $B_4 = \pi/2 = 1.570796\ldots$ for a two component order parameter. At a 3-dimensional tricritical point for a 1-component order parameter $B_4 = 2$ [20], and $B_4 = \Gamma(1/3)/\Gamma(2/3)^2 = 1.460998\ldots$ for a 2-component order parameter.

IV. SIMULATIONS AND RESULTS FOR $\mu_I < m_\pi$

We have simulated 2-flavor QCD on $8^3 \times 4$ lattices in the neighborhood of the finite temperature transition from hadronic matter to a quark-gluon plasma, for small values of the isospin (I_3) chemical potential μ_I. Here, small μ_I means $\mu_I < m_\pi$ so that, even at zero temperature, the system is in the normal phase, i.e., in the phase where there is no I_3-breaking charged pion condensate. We set $\lambda = 0$, since a finite λ is only needed when there is a possibility of spontaneous I_3 breaking. Simulations were performed at three different quark masses $m = 0.05, 0.1, 0.2$.

At the lowest quark mass $m = 0.05$ we performed simulations over a range of μ_I values $0 \le \mu_I \le 0.55$, where the highest μ_I value is only just below the critical μ_I above which a pion condensate forms at low temperature. (At this quark mass, our measurement of the zero temperature transition at $\beta = 5.2$ indicates that the phase transition occurs at $\mu_I = \mu_c \approx 0.57$.) The larger quark masses were chosen to allow an even larger range of μ_Is for the normal phase. For $m = 0.1$ we simulated over the range $0 \le \mu_I \le 0.7$ ($\mu_c \approx 0.81$), while for $m = 0.2$ we covered the range $0 \le \mu_I \le 1$ ($\mu_c \approx 1.14$). At each of the selected μ_I values we performed simulations over a range of $\beta = 6/g^2$ values spanning the finite temperature transition. We used a range of updating increments (in molecular-dynamics "time") for these simulations. These ranged from $dt = 0.1$ for $m = 0.1, 0.2$ and small μ_I down to $dt = 0.01$ for $m = 0.05$ and $\mu_I = 0.55$ close to the transition. For each quark mass we performed simulations as long as 20,000 molecular-dynamics time-units (trajectories) at individual values of (β, μ_I) close to a transition.

At each value of m, μ_I and β we measured the average plaquette, the Wilson Line (Polyakov Loop), the chiral condensate and the isospin density for each trajectory. For the fermionic quantities, where we calculate stochastic estimates, we used five noise vectors for each trajectory,

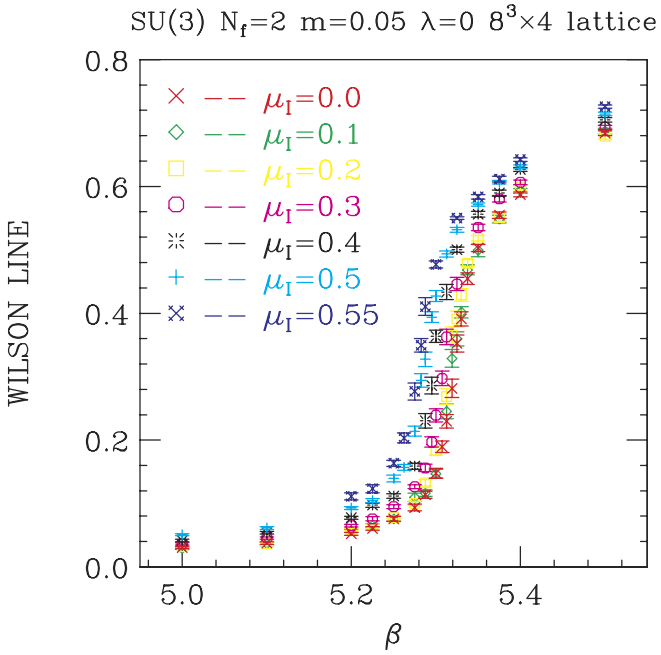

FIG. 2 (color online). Wilson Line as a function of β for various $\mu_I < m_\pi$ and $m = 0.05$.

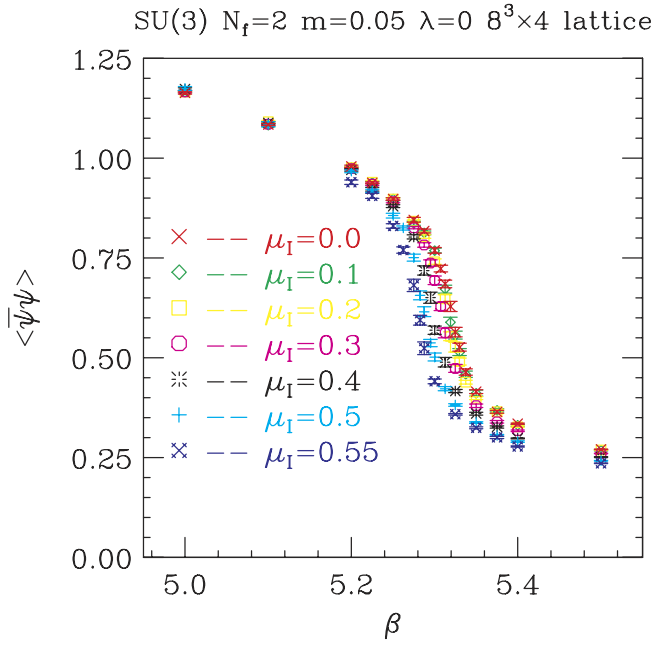

FIG. 3 (color online). $\langle\bar{\psi}\psi\rangle$ as a function of β for various $\mu_I < m_\pi$ and $m = 0.05$.

which enabled us to make unbiased estimates of the susceptibilities and Binder cumulants. Figure 2 shows the Wilson Line as a function of β for each μ_I at quark mass $m = 0.05$. Note that there is a rapid crossover marking the transition. In addition we see that the position of the crossover moves towards smaller β and hence lower temperature as μ_I is increased. However, we notice that the crossover β, β_c varies only slowly with μ_I. The corresponding values of the chiral condensate, $\langle\bar{\psi}\psi\rangle$ are given in Fig. 3. Again we see a rapid crossover close to the position of that for the Wilson Line. Figure 4 shows the behavior of the isospin density j_0^3 for the same mass and μ_Is. Here we see the finite temperature transition again. We note that the value of the isospin density in the quark-gluon plasma (high β) increases with increasing μ_I. At each μ_I it appears to level off at large β. Note that this is not the lattice artifact of saturation; j_0^3 in this domain is far below its saturation value of 3. The rise in j_0^3 occurs because increasing μ_I raises the Fermi surface. These observables for $m = 0.1$ and $m = 0.2$ behave very similarly to those for $m = 0.05$, except that the crossovers occur at larger β values as mass is increased.

The transitions we have observed in each of these masses and chemical potentials appear to be smooth crossovers rather than actual phase transitions, as is expected to be the case for $\mu_I = 0$ (we will present further evidence for this later in this section). The position of the transition is thus defined as the β value which maximizes a chosen susceptibility. (Such definitions and Ferrenberg-Swendsen reweighting are used by other groups, as are the Binder cumulant methods used below [4–7,19].) This is a reasonable definition only if the positions of the maxima of the susceptibilities for the various observables are close, at least in the infinite volume limit. The susceptibility for a chosen observable $\mathcal{O}$ is defined as

$$\chi_{\mathcal{O}} = V\langle\mathcal{O}^2 - \langle\mathcal{O}\rangle^2\rangle, \tag{10}$$

where V is the space-time volume of the lattice. Note that

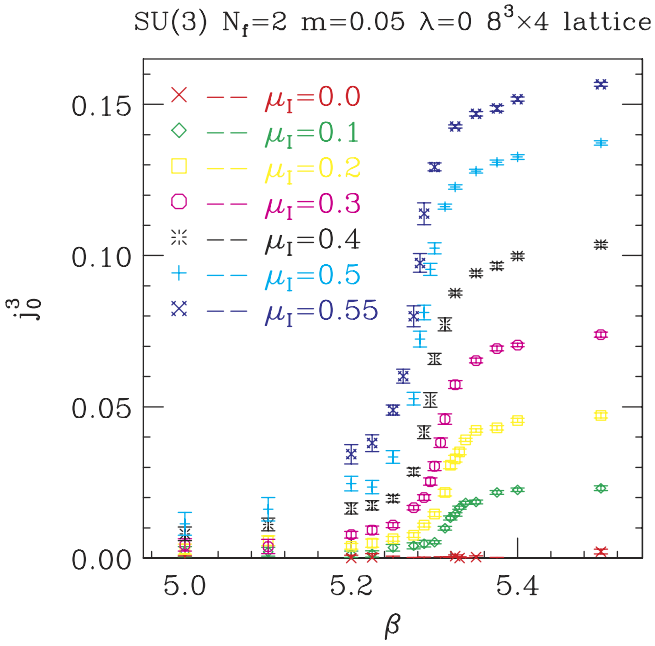

FIG. 4 (color online). j_0^3 as a function of β for various $\mu_I < m_\pi$ and $m = 0.05$.

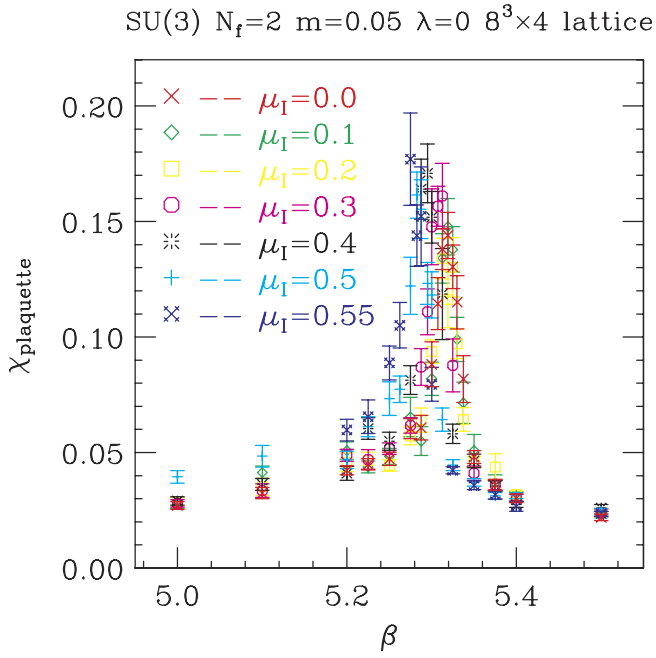

FIG. 5 (color online). Plaquette susceptibilities as functions of β for $\mu_I < m_\pi$, for $m = 0.05$.

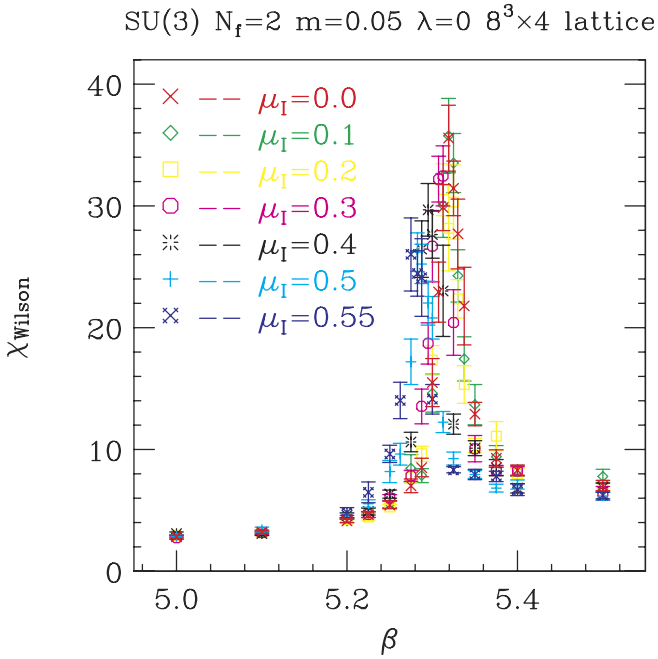

FIG. 6 (color online). Wilson line susceptibilities as functions of β for $\mu_I < m_\pi$, for $m = 0.05$.

this is the correct definition only for a local observable $\mathcal{O}$. We have also used this definition for the Wilson Loop which is only local in 3-space. Thus what we call χ_{Wilson} is strictly $N_t \chi_{\mathrm{Wilson}} = \chi_{\mathrm{Wilson}}/T$.

Figure 5 shows the plaquette susceptibilities for $m = 0.05$ at those βs at which we performed our simulations for each μ_I. These susceptibilities are clearly strongly peaked, and the peaks move to lower βs as μ_I is increased. Figure 6 gives the corresponding susceptibilities for the Wilson/Polyakov Line. Again these susceptibilities are strongly peaked and the peak moves to lower β as μ_I is increased. The main difference is that the peaks in these susceptibilities decrease slightly in height as μ_I is increased, whereas those for the plaquette susceptibilities increase with increasing μ_I. Figure 7 shows the susceptibilities for the chiral condensate, also for $m = 0.05$. By using all five stochastic estimators of $\langle\bar{\psi}\psi\rangle$ and removing the noise-diagonal contribution we obtain an unbiased estimate of this susceptibility These susceptibilities are the most strongly peaked of all the susceptibilities and the height of the peaks increases with increasing μ_I. Finally we show the susceptibilities for the isospin densities at $m = 0.05$ in Fig. 8. Again we used the five noise vectors to obtain an unbiased estimator. The rapid increase in the height of these peaks with increasing μ_I corresponds to the increase in j_0^3 seen in Fig. 4.

In order to pinpoint the susceptibility peaks more precisely, we use the distribution of observables and plaquette actions measured during our runs and use Ferrenberg-Swendsen reweighting [21] to estimate the susceptibilities at β values close to those at which we have performed simulations. If $\mathcal{O}$ is an observable for which $\mathcal{O}_i$, $i = 1, \ldots n$ are the measured values (lattice averaged), and $S_{\Box i}$ are the corresponding plaquette actions, at $\beta = \beta_0$, then

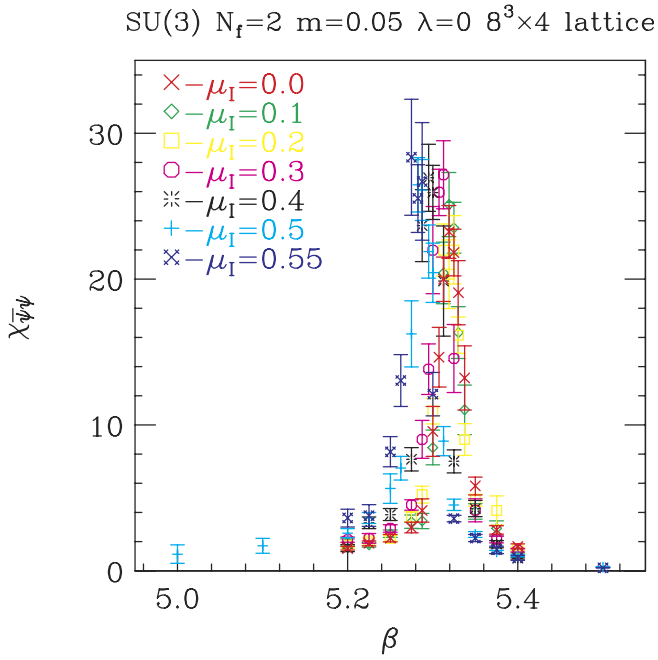

FIG. 7 (color online). $\bar{\psi}\psi$ susceptibilities as functions of β for $\mu_I < m_\pi$, for $m = 0.05$.

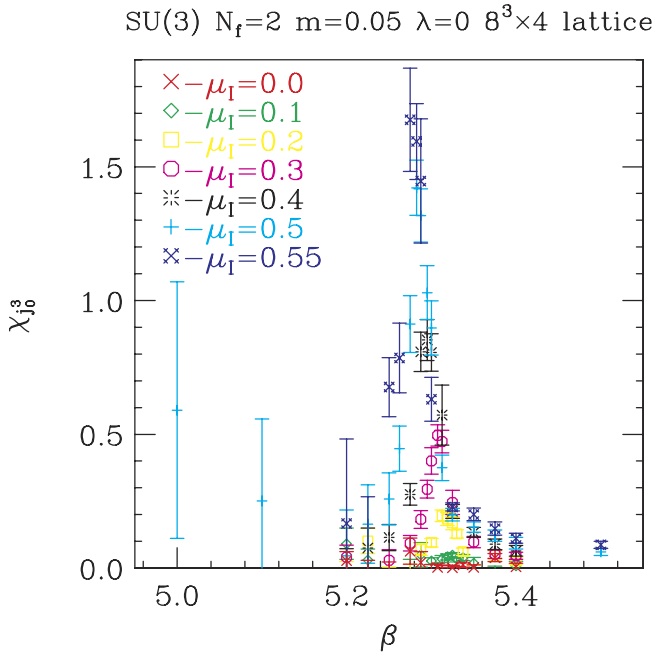

FIG. 8 (color online). Isospin density susceptibilities as functions of β for $\mu_I < m_\pi$, for $m = 0.05$.

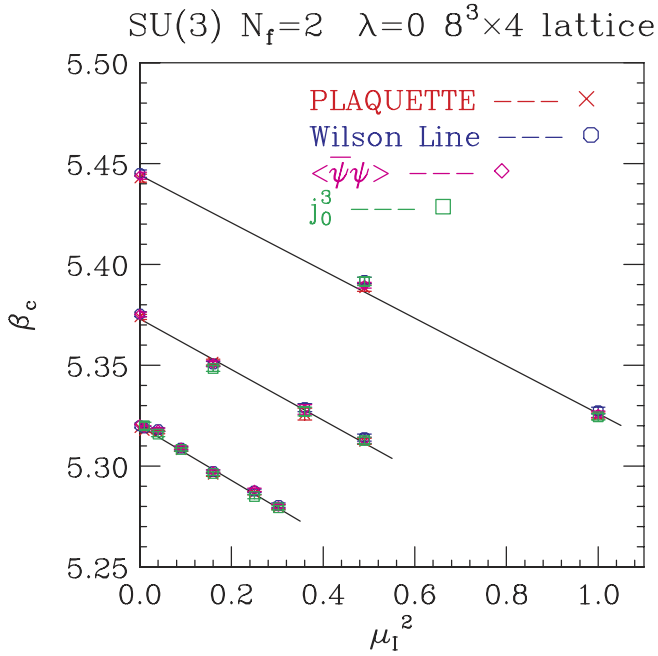

FIG. 9 (color online). β_c as functions of μ_I^2 together with straight line fits for each mass. The bottom set of points and line are for $m = 0.05$. The middle set of points and line are for $m = 0.1$. The top set of points and line are for $m = 0.2$.

$$\langle \mathcal{O} \rangle(\beta) = \frac{\sum_i \exp[-6V(\beta - \beta_0)S_{\Box i}]\mathcal{O}_i}{\sum_i \exp[-6V(\beta - \beta_0)S_{\Box i}]} \tag{11}$$

for β close enough to β_0 that the distributions of $S_\Box$ values at β and β_0 have significant overlap. Applying this formula to estimate both $\langle \mathcal{O} \rangle$ and $\langle \mathcal{O}^2 \rangle$ yields the desired susceptibility $\chi_\mathcal{O}$. Jackknife methods are used to determine the errors in both the susceptibilities and the positions of their peaks. It turns out that for our simulations at each m and μ_I, we have $3 - 5\beta$ values close enough to the peak β_c to be used to determine β_c. After checking that the estimates of β_c from each of these points are consistent, we obtain our final estimate as a χ^2 weighted average of these.

In Fig. 9 we plot our β_c estimates from each of the four susceptibilities as functions of μ_I^2 for all three masses. There is clearly good agreement between the β_c values obtained from the different susceptibilities. Arguments as to why this should be so have been presented in references [22–25]. Since for a fixed mass

$$\beta_c(\mu_I) = \beta_c(-\mu_I) \tag{12}$$

β_c is a function of μ_I^2. For $|\mu_I|$ is small enough it is also an analytic function of μ_I. Thus for small μ_I,

$$\beta_c(\mu_I) = a + b\mu_I^2 + c\mu_I^4 + \ldots \tag{13}$$

We have therefore fit β_c to the form $\beta_c(\mu_I) = a + b\mu_I^2$, for each mass. Choosing to fit the plaquette susceptibilities, we get

$$\begin{aligned} \beta_c &= 5.3198(9) - 0.134(6)\mu_I^2 \quad \text{for } m = 0.05 \\ \beta_c &= 5.3731(11) - 0.126(5)\mu_I^2 \quad \text{for } m = 0.1 \\ \beta_c &= 5.4443(27) - 0.118(4)\mu_I^2 \quad \text{for } m = 0.2. \end{aligned} \tag{14}$$

These lines are plotted in Fig. 9. Since χ^2/dof is 3.2 for $m = 0.05$, 1.1 for $m = 0.1$ and 2.4 for $m = 0.2$, these are not excellent fits. However, including the quartic term does not improve the $m = 0.05$ fit, and adding even more terms would be a meaningless exercise. If we use the 2-loop expression for the running of the coupling constant, we can convert Eq. (14) into equations for the μ_I dependence of T_c. At small μ_I, these have the form

$$\frac{T_c(\mu)}{T_c(0)} = 1 - C\left(\frac{\mu}{T}\right)^2, \tag{15}$$

where we have defined $\mu = \mu_I/2$. We estimate that $C \approx 0.043$ for $m = 0.05$, $C \approx 0.040$ for $m = 0.1$, $C \approx 0.038$ for $m = 0.2$ and $C \approx 0.049$ in the chiral limit. The use of "$\approx$" is to indicate that at these large couplings, the systematic error in using 2-loop running of the coupling constant for staggered quarks is undoubtably sizeable.

It was observed by the Bielefeld-Swansea group that at small μ and μ_I, the dependence of β_c on μ and on μ_I was identical within their errors [4]. In our notation this would mean that

$$\beta_c(\mu) = \beta_c(\mu_I = 2\mu). \tag{16}$$

This means that one can determine the position of the finite temperature transition for small μ by simulating

with the magnitude of the fermion determinant and ignoring the phase. Let us give an intuitive argument why this might be the case. If θ is the phase of the fermion determinant, and $\mathcal{O}$ is a gauge-field observable (such as the plaquette or Wilson line) then

$$\langle \mathcal{O} \rangle_\mu = \frac{\langle \exp(i\theta)\mathcal{O} \rangle_{\mu_I = 2\mu}}{\langle \exp(i\theta) \rangle_{\mu_I = 2\mu}}, \tag{17}$$

where for $\mathcal{O}$ real we can replace $\exp(i\theta)$ with $\cos(\theta)$. For the lattice size used by the Bielefeld-Swansea group, there was a range of μ over which this denominator was not too small and varied smoothly with μ and slowly with β, as β swept across the β_c. Here the denominator cannot be responsible for the transition. When the fluctuations in θ are so well-behaved, it is reasonable to treat $\exp(i\theta)\mathcal{O}$ as another observable. Since the position of the transition appears to be nearly independent of the chosen observable, this would suggest that the position of the transition would be the same for this new observable. If so, the smooth behavior of the denominator would imply that the position of the transition at finite μ should be the same as that for the transition at finite μ_I for $\mu_I = 2\mu$. It is also not unreasonable to assume that the nature of the two transitions might be the same. Such observations are not new (see, for example, [26]).

If the relation between $\beta_c(\mu)$ and $\beta_c(\mu_I)$ holds with the standard staggered action (the Bielefeld-Swansea group used the p-4 action) we can compare our formulae for $\beta_c(\mu_I)$ (Eq. (14)) with that obtained by de Forcrand and Philipsen [6]

$$\beta_c = 5.2865(18) - 0.149(10)\mu_I^2 \quad \text{for } m = 0.025, \tag{18}$$

where we have made the substitution $\mu = \mu_I/2$ in their equation. This would appear to be consistent with our equations, taking into account the difference in mass. To examine whether this agreement is quantitative, we fit Eqs. (14) and (18) to the expected scaling form

$$\begin{aligned} \beta_c(m, \mu_I) &= \beta_c(m, 0) - a(m)\mu_I^2 \\ \beta_c(m, 0) &= \beta_c(0, 0) + bm^{1/\beta_m\delta} \\ a(m) &= a(0) - cm^{1/\beta_m\delta}. \end{aligned} \tag{19}$$

Such scaling fits have been considered by [27,28] at zero chemical potentials. For the expected continuum $O(4)$ scaling $1/\beta_m\delta \approx 0.55$, while for the lattice $O(2)$ scaling $1/\beta_m\delta \approx 0.59$. [Note that such scaling is only derivable for the case of finite μ, where, in the chiral limit, the line of crossovers becomes a line of second-order transitions in the same universality class as the $\mu = 0(\mu_I = 0)$ transition. We are using the assumed relationship between finite μ and finite μ_I to extend it to finite μ_I.] The fit of all four equations to $O(4)$ scaling gives $\beta_c(0, 0) = 5.210(3)$, $b = 0.57(1)$, with a $\chi^2/dof = 1.6$, and $a(0) = 0.152(6)$, $c = 0.085(19)$ with a $\chi^2/dof = 0.5$. The fit to $O(2)$ scaling gives $\beta_c(0, 0) = 5.219(3)$, $b = 0.59(2)$ with a $\chi^2/dof = 2.4$ and $a(0) = 0.151(6)$, $c = 0.087(20)$ with a $\chi^2/dof = 0.5$. Considering the quality of the fits in Eq. (14), we consider either of these scaling fits to be good enough to support our claim that we are consistent with de Forcrand and Philipsen, and that the combined measurements are consistent with the expected scaling with quark mass m. Note that our value of $\beta_c(0, 0)$ is less than that obtained in [27,28]. We should not expect good agreement with the later paper, since it uses a larger lattice and finite size effects are non-negligible on an $8^3 \times 4$ lattice. The fit in the earlier work was over the mass range $0.02 \leq m \leq 0.075$, while ours was over the range $0.025 \leq m \leq 0.2$. Considering the rapid variation of the scaling form at small m, the difference between our result, 5.210(3) and their's, 5.222(3) is perhaps not surprising.

What remains to be checked is that the phase (θ) of the fermion determinant is well-behaved. Since calculating the fermion determinant is very expensive, we use the series expansion for θ given in [4]. In our normalization,

$$\theta = \frac{1}{4}\mu_I V \mathrm{Im}(j_0) + \mathcal{O}(\mu_I^3), \tag{20}$$

where j_0 is the number density normalized to four flavors (1 staggered fermion field). We use our five stochastic estimators/configuration of j_0 to obtain an unbiased estimator of $\langle \theta^2 \rangle$ through order μ_I^2. (We also made an unbiased estimator of $\langle j_0^4 \rangle$ which had a poor enough signal/noise ratio that we did not even try to estimate $\langle \theta^4 \rangle$ or the higher order contributions to $\langle \theta^2 \rangle$.) Our results for a range of β values which span the $\mu_I = 0$ transition for each quark mass are given in Table I. A reasonable measure of how "well-behaved" this phase is, is $\langle \cos(\theta) \rangle$. When this

TABLE I. Fluctuations in the phase of the fermion determinant.

m	β	$\langle [\mathrm{Im}(j_0)]^2 \rangle$	$\langle \theta^2 \rangle / \mu_I^2$
0.05	5.3000	$2.1(8) \times 10^{-5}$	5.5(2.1)
0.05	5.3075	$2.6(8) \times 10^{-5}$	6.7(1.7)
0.05	5.3125	$1.0(5) \times 10^{-5}$	2.6(1.2)
0.05	5.3190	$2.1(5) \times 10^{-5}$	5.5(1.2)
0.05	5.3250	$1.5(4) \times 10^{-5}$	4.0(1.2)
0.05	5.3300	$1.0(5) \times 10^{-5}$	2.7(1.2)
0.05	5.3375	$1.0(3) \times 10^{-5}$	2.7(0.9)
0.10	5.3500	$1.6(4) \times 10^{-5}$	4.1(1.2)
0.10	5.3625	$1.8(3) \times 10^{-5}$	4.7(0.8)
0.10	5.3750	$1.3(3) \times 10^{-5}$	3.3(0.7)
0.10	5.3875	$0.6(2) \times 10^{-5}$	1.5(0.6)
0.10	5.4000	$0.2(7) \times 10^{-5}$	0.6(1.8)
0.20	5.4250	$1.7(2) \times 10^{-5}$	4.4(0.6)
0.20	5.4375	$1.2(2) \times 10^{-5}$	3.2(0.5)
0.20	5.4500	$1.0(2) \times 10^{-5}$	2.5(0.4)
0.20	5.4625	$0.7(1) \times 10^{-5}$	1.9(0.4)
0.20	5.4750	$0.7(2) \times 10^{-5}$	1.9(0.5)

quantity is close to 1, the oscillations in phase are small, and it is reasonable to produce ensembles with the magnitude of the determinant and to include the phase in the measurement. When this expectation value falls towards zero, θ is almost uniformly distributed over the interval $(-\pi, +\pi]$, and the contributions of configurations generated using the magnitude of the determinant can easily cancel, as they would in the denominator of Eq. (17) for this case. How small $\langle\cos(\theta)\rangle$ can get before generating ensembles without the phase becomes invalid is a matter of "experimentation", but one might expect that $\langle\cos(\theta)\rangle > 0.5$ would be a reasonable range over which we could use this method. To the order in μ_I to which we work we must take $\cos(\theta) \approx 1 - \frac{1}{2}\theta^2$. Applying our criterion to the measurements of Table I, we see that, even in the worst case, we should be able to trust the relationship between measurements at finite μ_I and finite μ, out to $\mu_I^2 \approx 0.15$, i.e., out to $\mu_I \approx 0.4$. Thus it is not unreasonable to assume that this relation will be a reasonable approximation for most of the region $\mu_I < m_\pi$.

Let us now examine the nature of these transitions more closely. We have observed that the transitions appear smooth in all measured observables. This suggests that they are merely rapid crossovers. Histogramming those observables which could show discontinuities if there were a first-order transition, shows a single broad peak for all masses considered for all $\mu_I < m_\pi$, which suggests a crossover (or possibly a second-order transition) but not a first-order transition. We note that on such small lattices, one can observe a double peak structure, even where the transition is a crossover or second-order transition. However, it is rare that a first-order transition would not show a double peak, unless it were very weak. In Fig. 10 we show histograms of the Wilson Line (Polyakov Loop) for $m = 0.05$ at an intermediate value of μ_I (0.3) and one close to m_π (0.55). These both show a single broad peak as advertised, and are typical. [We chose to show the Wilson Line rather than the chiral condensate, since use of stochastic estimators (even after averaging over all five estimates for each configuration) could possibly obscure a double peak.]

Finally, we have calculated the fourth-order Binder cumulants B_4 for the chiral condensate at the transition for each m and μ_I. Having five noisy estimators per configuration, we were able to generate an unbiased estimator for B_4. We again use Ferrenberg-Swendsen reweighting to interpolate between those β values at which we ran our simulations. We determined the position of the transition for each m and μ_I as that β which minimized B_4. This method of determining the position of the transition gave β_c values in excellent agreement with those obtained from the maxima of the corresponding susceptibilities. We plot these B_4 values in Fig. 11.

If there were a critical endpoint, which is expected to be in the Ising universality class, we would expect B_4 to pass through its Ising value, $B_4 = 1.604$, at this endpoint. For the crossover region, B_4 should lie above the Ising value, approaching 3 in the limit of large lattices. In the first-order domain (if it existed) B_4 should lie below the Ising value, approaching 1 in the large lattice limit. We have plotted the Ising value as a dashed line in Fig. 11. Clearly B_4 lies well above 1.604 and shows no sign of approaching this value. Hence the evidence from Binder

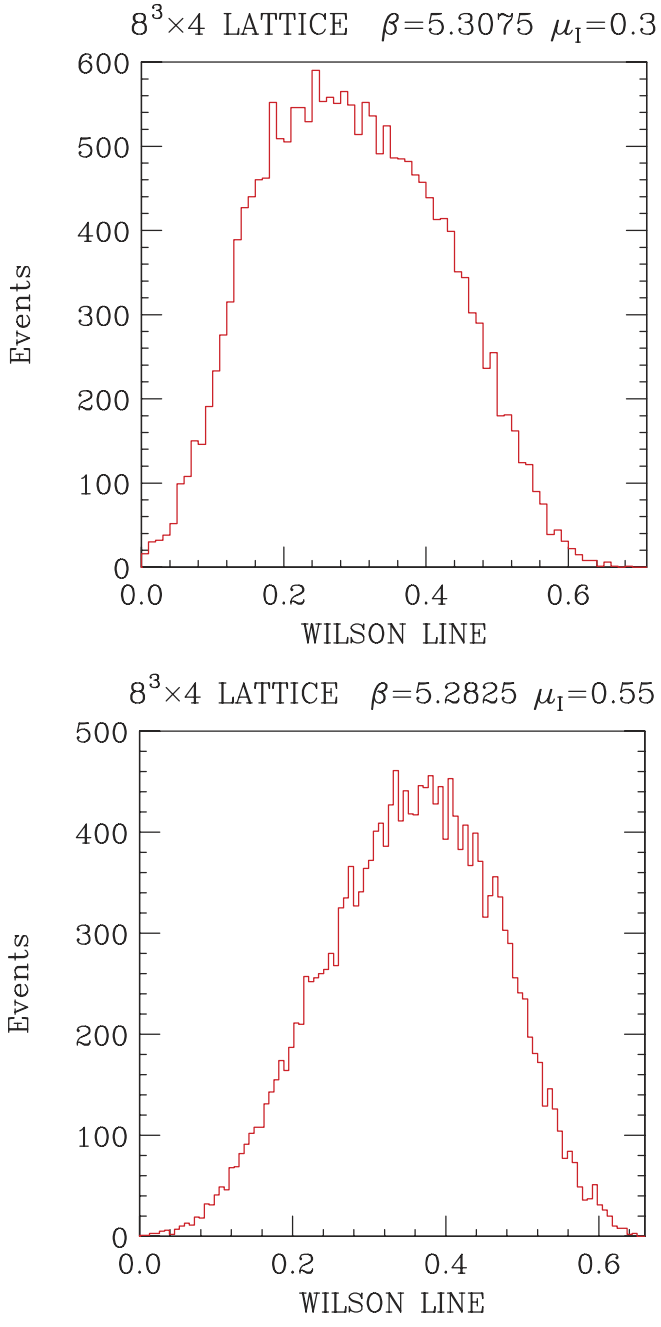

FIG. 10 (color online). Histograms of distribution of Wilson Line values for $m = 0.05$: (a) For $\mu_I = 0.3$, $\beta = 5.3075$; (b) For $\mu_I = 0.55$, $\beta = 5.2825$.

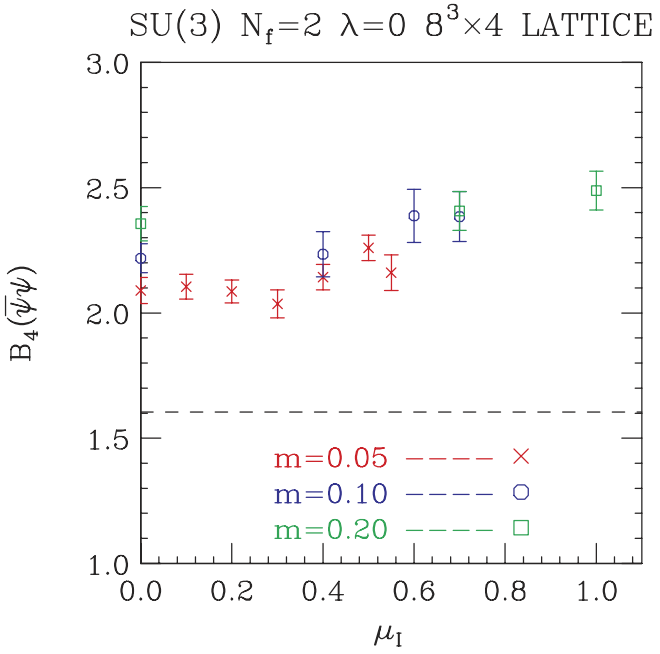

FIG. 11 (color online). Fourth-order Binder cumulants (B_4) for $\langle\bar{\psi}\psi\rangle$ as a function of μ_I. The dashed line is at $B_4 = 1.604$, the value for the 3-dimensional Ising model.

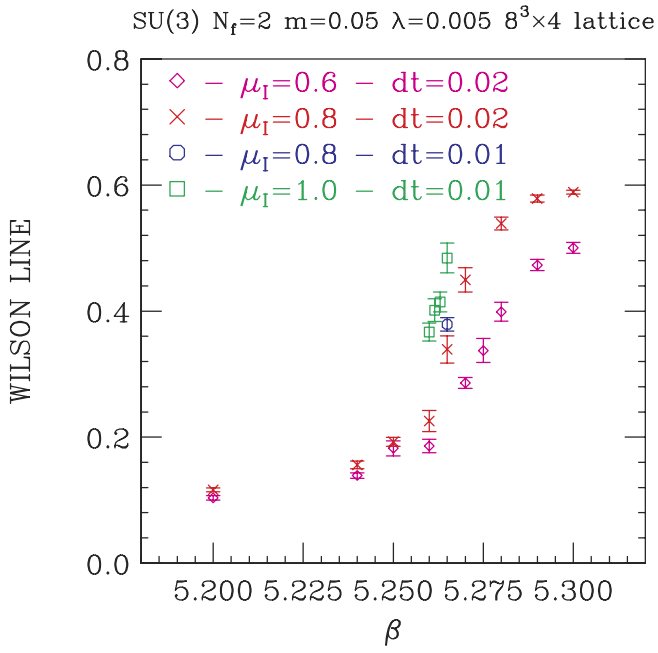

FIG. 12 (color online). Wilson Line (Polyakov Loop) for large μ_I on an $8^3 \times 4$ lattice with $m = 0.05$ and $\lambda = 0.005$

cumulants supports our conclusion that the transition is a crossover for all $\mu_I < m_\pi$, over a range of quark masses.

V. SIMULATIONS AND RESULTS FOR $\mu_I > m_\pi$

In the region where $\mu_I > m_\pi$, for $\lambda = 0$, the charged pion condensate evaporates at the finite temperature transition and I_3 symmetry, which is broken spontaneously at low temperature, is restored. Hence, this finite temperature transition is a true phase transition. However, since in this case the low temperature phase has a true Goldstone mode, this would render the Dirac operator singular (at least in the large volume limit). Hence we must use a nonzero λ, which we keep small so that we can infer information about the $\lambda \to 0$ limit. For $\lambda \neq 0$, the phase transition is no longer required, and our earlier work indicates that for μ_I just above m_π, the transition is softened to a crossover. We can now search for a critical endpoint in the high μ_I ($\mu_I > m_\pi$) regime. Again the critical endpoint would be expected to lie in the universality class of the 3-dimensional Ising model. For μ_I above this endpoint the transition would be first-order. Unfortunately, in this domain, we cannot argue that the finite μ_I and the finite μ transitions are related.

We have performed simulations on an $8^3 \times 4$ lattice at quark mass $m = 0.05$ and $\lambda = 0.005$, at $\mu_I = 0.6$, $\mu_I = 0.8$ and $\mu_I = 1.0$. The $\mu_I = 0.8$ simulations were repeated on a $16^3 \times 4$ lattice. In Fig. 12, we show the behavior of the Wilson Lines as functions of β for the three μ_I values from our simulations on an $8^3 \times 4$ lattice. At $\mu_I = 1.0$ we have only performed simulations very close to the transition. We obtained the high statistics needed to reveal the true nature of this transition at those β values closest to the transition for each μ_I—for $\mu_I = 0.6$ we obtained 40 000 time-units at $\beta = 5.27$, for $\mu_I = 0.8$ we obtained 40 000 time-units at $\beta = 5.265$ using $dt = 0.02$ and a further 40 000 time-units using $dt = 0.01$, while at $\mu_I = 1.0$ we obtained 40 000 time-units at $\beta = 5.263$. We show histograms of the Wilson Line at these β and μ_I values in Fig. 13. At $\mu_I = 0.6$, the histogram shows no structure to suggest anything but a crossover, which would then become a second-order transition as $\lambda \to 0$. By $\mu_I = 0.8$ we begin to see clear signs of double peak suggestive of a 2-state signal. The signs of a double peak and a 2-state signal persist at $\mu_I = 1.0$.

Since lattices as small as $8^3 \times 4$ can show signs of a 2-state signal at a second-order transition or even a crossover, we need to examine this transition more closely. For this reason we have performed simulations on a $16^3 \times 4$ lattice at $\mu_I = 0.8$. Figure 14 shows the Wilson Line and the pion condensate from these simulations as functions of β. The reason dt was decreased from 0.02 to 0.01 close to the transition was that finite dt effects at $dt = 0.02$, both here and in our $8^3 \times 4$ runs at the same μ_I, can artificially enhance the 2-state signal. $dt = 0.01$ appears free from such enhancements. The reason for such behavior is that one effect of using a finite dt is to shift the effective β, measured from the kinetic energies using the equipartition theorem, to a value lower than the input β. This shift is larger below the transition than above. For $dt = 0.02$ below the transition, this shift is large enough that the distribution of effective βs has only a small

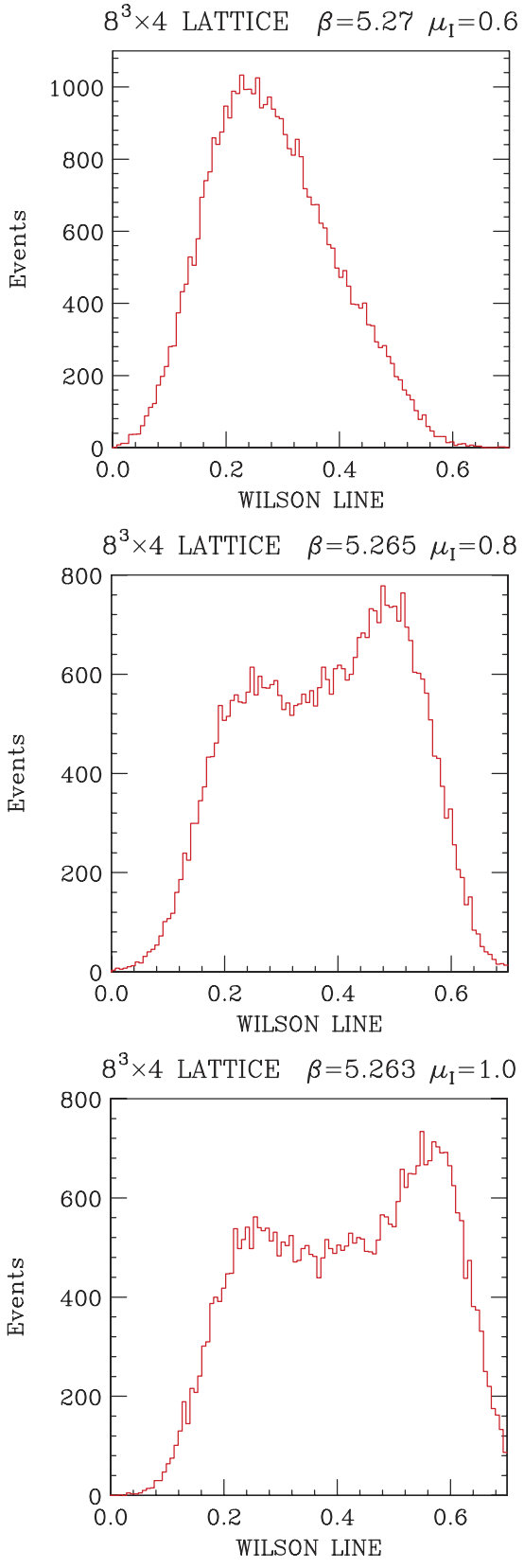

FIG. 13 (color online). Wilson Line histograms for large μ_I on an $8^3 \times 4$ lattice with $m = 0.05$ and $\lambda = 0.005$. (a) $\mu_I = 0.6$, $\beta = 5.27$; (b) $\mu_I = 0.8$, $\beta = 5.265$, $dt = 0.1$; (c) $\mu_I = 1.0$, $\beta = 5.263$.

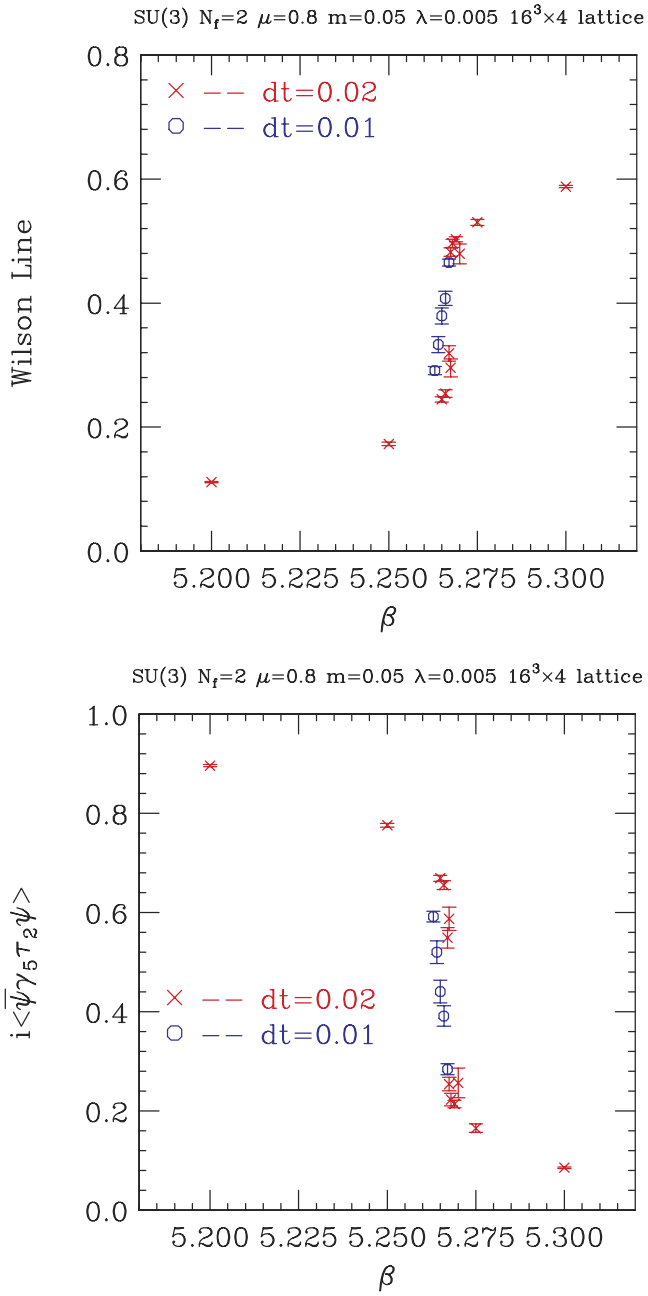

FIG. 14 (color online). (a) Wilson Line as a function of β at $\mu_I = 0.8$ on a $16^3 \times 4$ lattice. (b) Charged pion condensate as a function of β at $\mu_I = 0.8$ on a $16^3 \times 4$ lattice.

overlap with the input β. This impedes tunneling from below the transition to above the transition where the shift is much smaller. For $dt = 0.01$ the shift is smaller and the distribution of effective βs always has appreciable overlap with the input β. Hence we do not expect a significant suppression of tunneling leading to false first-order signals at this dt. For our $dt = 0.01$ runs at $\beta = 5.263$, $\beta = 5.264$ and $\beta = 5.265$ we ran for 30 000 time-units per β to obtain adequate statistics (for $\beta = 5.266$ and $\beta = 5.267$ we ran for 20 000 time-units per β).

Figure 15 shows a histogram of the Wilson Line values from our $\beta = 5.265$ runs. Although there is some double peak structure, the peaks are considerably closer together than they were for the $8^3 \times 4$ lattice, a sign that the double peak structure is a finite volume artifact and not the sign of a true 2-state signal indicating a first-order transition.

To clarify the situation we again turn to fourth-order Binder cumulants. Here the obvious choice is to look at the Binder cumulants of the pion condensate, since this is the order parameter of this transition in the $\lambda \to 0$ limit. We plot B_4 versus μ_I in Fig. 16 obtained using Ferrenberg-Swendsen reweighting to obtain B_4 at that β which minimizes B_4 for that particular value of μ_I. The $8^3 \times 4$ points suggest that the Binder cumulant crosses the Ising value somewhere above $\mu_I = 0.8$ and probably close to $\mu_I = 1.0$. If so, this would indicate that there is a critical end point with Ising critical exponents at $\mu_I = \mu_c$ with $\mu_c \sim 1.0$. For $\mu_I > \mu_c$ the transition would become first-order. The $16^3 \times 4$ Binder cumulant at $\mu_I = 0.8$ is large enough to indicate that μ_c is indeed greater than 0.8. We would expect that if the transition is first-order for $\lambda = 0.005$ it will also be first-order for $\lambda = 0$. Hence there will be a tricritical point for $\mu_I = \mu_t$ where $\mu_t < \mu_c$. Since $\lambda = 0.005$ is rather small, we expect that $\mu_t \approx \mu_c$.

Finally, let us note that the position of the transition at $\mu_I = 0.6$ is consistent with Eq. (14). The position of the transitions at $\mu_I = 0.8$ and $\mu_I = 1.0$ lie above this prediction. β_c does, however, continue to decrease with increasing μ_I for $\mu_I > m_\pi$, just not as fast. This suggests

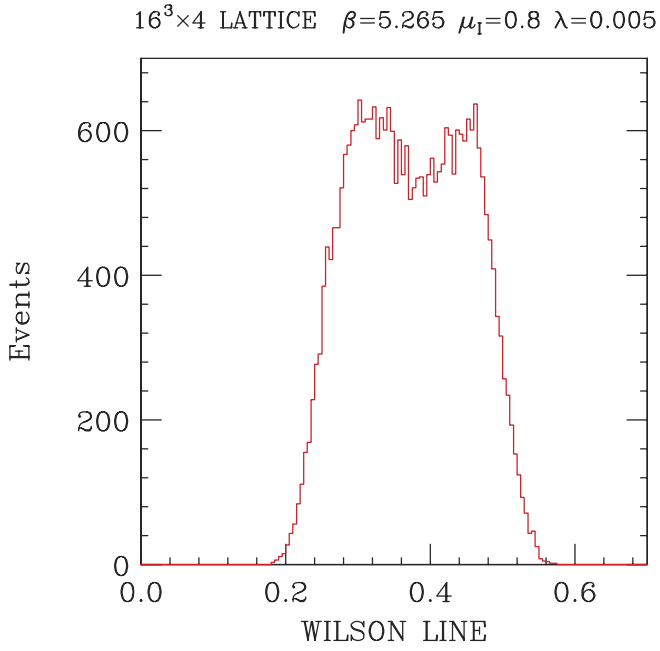

FIG. 15 (color online). Histogram of Wilson line values close to the transition on a $16^3 \times 4$ lattice at $\mu_I = 0.8$ ($\beta = 5.265$).

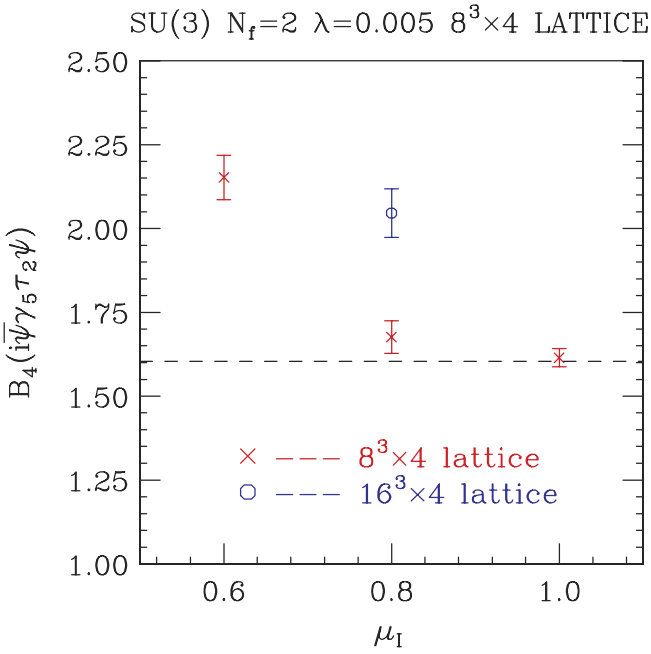

FIG. 16 (color online). Binder cumulants of the charged pion condensate, $i\langle\bar{\psi}\gamma_5\tau_2\psi\rangle$, as functions of μ_I

the scenario in Fig. 1 where the line of finite temperature crossovers for $\mu_I < m_\pi$ continues as a line of finite temperature phase transitions for $\mu_I > m_\pi$ for $\lambda = 0$. For small λ the second-order transitions will soften to crossovers since the pion condensate is no longer a true order parameter, the tricritical point will become a critical endpoint, and the first-order line will survive.

VI. CONCLUSIONS

We have simulated lattice QCD with two flavors of staggered quarks ("half" a staggered quark field) with a chemical potential μ_I for isospin (I_3), in the neighborhood of the finite temperature transition. For $\mu_I < m_\pi$ we have determined the μ_I dependence of β_c, the transition $\beta = 6/g^2$, for each of three quark masses. We have noted that the fluctuations of the phase of the fermion determinant on an $8^3 \times 4$ lattice are well enough behaved for small μ_I that there should be a range of μ_I for which the dependence of β_c, and hence temperature, on μ_I and on the quark-number chemical potential μ should be identical for $\mu_I = 2\mu$, as was observed previously by the Bielefeld-Swansea group for the p-4 action [4].

What we find is that β_c falls slowly with increasing μ_I. This falloff is approximately linear in μ_I^2 over the whole $\mu_I < m_\pi$ region. The value of β_c at $\mu_I = 0$ increases with mass and the falloff with increasing μ_I^2 becomes less steep as the mass is increased. This dependence on mass is small. We have taken the results of de Forcrand and Philipsen [6] and converted them from a μ dependence to a μ_I dependence. Since these were calculated at a smaller

mass $m = 0.025$ than ours, we cannot compare them directly. We fit the mass dependence of our "data" and theirs (a total of four different masses) to that expected from critical scaling with both the continuum $O(4)$, and lattice $O(2)$ universality classes, as was done at zero chemical potential in [27,28]. Both these fits prove acceptable. This is a direct confirmation that the μ_I and μ dependence of the transition temperature are the same, at low chemical potentials.

Since the phase of the fermion determinant is an extensive quantity, the fluctuations in this phase increase with volume. This would suggest that the relation between finite μ and finite μ_I transitions would fail as the spatial volume is increased (the temporal extent is fixed at $1/T$), which is disturbing since the infinite volume limit is of the most physical importance. We suggest that the relevant phase to consider in establishing this relationship is not that on an arbitrarily large lattice, but is rather the phase on a lattice whose spatial size is of the order of the correlation length. Then we could limit our considerations of phase fluctuations to a modest lattice size, unless we were very close to a critical point.

It is worthwhile quantifying what we mean when we say that the dependence on μ_I is slow, and what this means for the physical quantity, temperature. If we assume that the transition temperature at $\mu_I = \mu = 0$ is $T_c \approx 173$ MeV, then for our $m = 0.05$ simulations, 2-loop running of the coupling would imply that by $\mu_I = 0.55$ or in physical units $\mu_I \approx 362$ MeV ($\mu \approx 181$ MeV), the transition temperature will have fallen to $T_c \approx 164$ MeV. The relevance of this is even more clear when one considers that this latter μ value is an order of magnitude larger than those chemical potentials believed accessible by RHIC.

The smoothness of the transitions for $\mu_I < m_\pi$ for all three masses, and the absence of any sign of a 2-state signal strongly suggests that there is no critical endpoint, beyond which the transition would become first-order, in this domain. Analysis of the 4-th order Binder cumulant for each of the transitions, yields values $\gtrsim 2$. Since this quantity should pass through the 3-d Ising value 1.604(1) at a critical endpoint and lie below this value in the first-order region, this validates our assumption that the finite temperature transition from hadronic matter to a quark-gluon plasma remains a crossover throughout this region, and suggests that there is no critical endpoint for the corresponding range of μ.

We have also studied $\mu_I > m_\pi$, where the finite temperature transition for symmetry breaking parameter $\lambda = 0$ is a true phase transition from a pion condensed superfluid to a quark-gluon plasma. Here we have performed simulations with a small λ $(0.1m)$, where the second-order transition for μ_I just above m_π, softens to a crossover. We see evidence that for μ_I sufficiently large (~ 1), there is a critical endpoint, where the 4-th order Binder cumulant passes through its 3-d Ising value, and beyond which it is first-order. This observation needs to be confirmed on larger lattices, where the passage through the critical endpoint is expected be considerably more rapid. Unfortunately, in this regime, we cannot argue that a critical endpoint in μ_I is in any way related to a corresponding critical endpoint in μ.

We have recently begun to extend this work to the 3-flavor case. Not only is this more physical, but one can argue that it is possible to tune the critical endpoint to be as close to $\mu_I = 0$ as one desires, by careful choice of the quark mass m. In particular we can choose the critical value $\mu_I = \mu_c$ to obey $\mu_c < m_\pi$, and lie in the domain where the μ and μ_I transitions are related. Studies of the 3 and $2 + 1$ flavor transitions by various methods have located such a critical endpoint, but their predictions of its location are not in agreement [3,5,7]. Hence we have a chance to clarify the situation by a more direct approach.

It has been pointed out by de Forcrand, Kim and Takaishi [29], that simulating with finite μ_I provides a better ensemble for reweighting methods for finite μ, than simulations with zero chemical potential. Combined with our observations, this suggests that such reweighting would be optimal close to the finite temperature transition for small μ, and could be expected to give good predictions for observables in this domain. This should enable us to determine the equation-of-state in this low-μ domain. Of course, such reweighting requires calculating the phase of the fermion determinant. Doing this precisely would be prohibitively expensive for all but the smallest lattices. New methods for approximating the fermion determinant show promise for making these reweighting methods practical [30].

ACKNOWLEDGMENTS

D. K. S is supported under US Department of Energy, Division of High Energy Physics, contract W-31-109-ENG-38. J. B. K is supported in part by a National Science Foundation grant No. NSF PHY03-04252. The simulations described in this paper were performed on the IBM SP, Seaborg, at NERSC, the Jazz Linux PC cluster at the LCRC, Argonne National Laboratory, and Linux PCs belonging to the HEP Division at Argonne National Laboratory. One of us (D. K. S) would like to thank Philippe de Forcrand for helpful discussions about their work, its relationship to that of the Bielefeld-Swansea group and on the utility of Binder cumulant analyses of transitions. He would also like to thank Simon Hands for discussions of the work of the Bielefeld-Swansea group.

[1] Z. Fodor and S. D. Katz, Phys. Lett. B **534**, 87 (2002).
[2] Z. Fodor and S. D. Katz, J. High Energy Phys. 03, (2002) 014.
[3] Z. Fodor and S. D. Katz, J. High Energy Phys. 04, (2004) 050.
[4] C. R. Allton *et al.*, Phys. Rev. D **66**, 074507 (2002).
[5] F. Karsch, C. R. Allton, S. Ejiri, S. J. Hands, O. Kaczmarek, E. Laermann, and C. Schmidt, Nucl. Phys. B, Proc. Suppl. **129**, 614 (2004).
[6] P. de Forcrand and O. Philipsen, Nucl. Phys. B **642**, 290 (2002).
[7] P. de Forcrand and O. Philipsen, Nucl. Phys. B **673**, 170 (2003).
[8] M. D'Elia and M. P. Lombardo, Phys. Rev. D **67**, 014505 (2003).
[9] R. V. Gavai and S. Gupta, Phys. Rev. D **68**, 034506 (2003).
[10] R. Gavai, S. Gupta and R. Roy, Prog. Theor. Phys. Suppl. **153**, 270 (2004).
[11] V. Azcoiti, G. Di Carlo, A. Galante, and V. Laliena, hep-lat/0409160; hep-lat/0409158.
[12] D. T. Son and M. A. Stephanov, Phys. Rev. Lett. **86**, 592 (2001).
[13] D. T. Son and M. A. Stephanov, Phys. At. Nucl. **64**, 834 (2001); [Yad. Fiz. **64**, 899 (2001)].
[14] J. B. Kogut and D. K. Sinclair, Phys. Rev. D **66**, 034505 (2002).
[15] J. B. Kogut and D. K. Sinclair, Nucl. Phys. B, Proc. Suppl. **119**, 556 (2003).
[16] J. B. Kogut and D. K. Sinclair, Nucl. Phys. B, Proc. Suppl. **129**, 542 (2004).
[17] D. K. Sinclair, J. B. Kogut, and D. Toublan, Prog. Theor. Phys. Suppl. **153**, 40 (2004).
[18] K. Binder, Z. Phys. B **43**, 119 (1981).
[19] F. Karsch, E. Laermann, and C. Schmidt, Phys. Lett. B **520**, 41 (2001).
[20] A. Lipowski and M. Droz, Phys. Rev. E **66**, 016118 (2002).
[21] A. M. Ferrenberg and R. H. Swendsen, Phys. Rev. Lett. **61**, 2635 (1988).
[22] Y. Hatta and K. Fukushima, Phys. Rev. D **69**, 097502 (2004).
[23] K. Fukushima, Phys. Rev. C **67**, 025203 (2003).
[24] A. Mocsy, F. Sannino and K. Tuominen, Phys. Rev. Lett. **91**, 092004 (2003).
[25] A. Mocsy, F. Sannino and K. Tuominen, Phys. Rev. Lett. **92**, 182302 (2004).
[26] T. Takaishi, Prog. Theor. Phys. Suppl. **153**, 277 (2004).
[27] F. Karsch and E. Laermann, Phys. Rev. D **50**, 6954 (1994).
[28] F. Karsch, E. Laermann, and A. Peikert, Nucl. Phys. B **605**, 579 (2001).
[29] P. de Forcrand, S. Kim, and T. Takaishi, Nucl. Phys. B, Proc. Suppl. **119**, 541 (2003).
[30] K. F. Liu, Int. J. Mod. Phys. B **16**, 2017 (2002).